Preprints of the 21st IFAC World Congress (Virtual)
Berlin, Germany, July 12-17, 2020

Integration of PD-type Iterative Learning Control with Adaptive Sliding Mode Control

Armin Norouzi * **Charles Robert Koch** *

* *Mech. Dept. Engineering, University of Alberta*
(e-mail: norouziy@ualberta.ca, bob.koch@ualberta.ca)

Abstract: Proportional-Derivative type Iterative Learning Controller (PD-ILC) is combined with an Adaptive Sliding Mode Controller (ASMC) using a plug-in structure to a rotary pendulum. The ASMC adaptation law is used to update a switching gain of sliding surface in Sliding Mode Control (SMC) controller. The proposed hybrid controller stability and convergence are mathematically shown and then experimentally demonstrated using two-degree-of-freedom (2-DOF) Quanser© QUBE^{TM} Servo 2 Rotary Pendulum. Results illustrate that adaptation law helps the controllers to achieve higher accuracy tracking performance compared to the classic SMC controller. Based on the experimental results, the hybrid control of PD-ILC and ASMC has faster and more accurate tracking results than ILC controller indicating the combined controller has better performance than the individual controllers.

Keywords: Iterative Learning Control; Sliding Mode Control; Adaptive Control; Robotic Pendulum; Hybrid Control

1 Introduction

Iterative Learning Control (ILC) is a control method that uses previous cycle information to learn how to control a system which has repetitive dynamics (Owens, 2015). For example in the industrial automation robotic manipulators repeat a certain action or motion. Each repeating action is called a "cycle," and the ILC controller uses error and control input from the previous cycle to learn the control input of upcoming cycle. The learning procedure in ILC is similar to humans learning a task where they gain skill by repeating it. Learning a new language is an example of skills that humans learn by repeating it over time. ILC has a simple structure which is computationally inexpensive and easy to design. Also, the model-free design has low complexity which is useful for real-time implementation and when it is difficult to model the system with high accuracy. Additionally, it has the potential to achieve perfect tracking by using a "non-causal" control signal (Xu et al., 2008).

Different types of ILC controllers have been used in literature such as proportional type ILC (P-type ILC) (Slepicka and Koch, 2016), proportional-derivative type (PD-type ILC) (Liu and Ruan, 2018), and proportional-integral-derivative type (PID-type ILC) (Kim and Kim, 1996). ILC has been implemented on a wide variety of systems. Dual-loop D-type ILC law was used to control a flapping wing Micro Aerial Vehicle under distributed disturbances (He et al., 2018). ILC was designed for a class of nonlinear uncertain system, and the convergence of the controller was analyzed based on composite energy function (Xu et al., 2004). PD-type ILC was used to control a Multiple Flexible Manipulator Robot System, and the results showed that PD-type ILC is an effective method to obtain exact reference tracking (Dong et al., 2019). Adding a fuzzy mechanism to a PD-type ILC increased convergence speed of ILC and generalized it to be useful for different plants (Norouzi and Koch, 2019) and (Norouzi et al., 2019a). Error-tracking iterative learning control was used to control a robot manipulator with random initial errors (Yan et al., 2019). In addition, ILC can be combined with conventional controllers as a plug-in hybrid controller to improve the performance of conventional controllers. Learning-based control using norm-optimal iterative learning control with embedded PID controller was used to control soft robotic arm (Hofer et al., 2019).

Sliding Mode Controller (SMC) is a Lyapunov based controller which is designed based on the nonlinear system model (Khalil, 2002). This controller is robust and can overcome system uncertainty and input disturbances (Norouzi et al., 2019b). SMC was combined with different control laws such as adaptive control (Norouzi et al., 2018), Backstepping Control (Norouzi et al., 2019d), and Fuzzy Control (Jiang et al., 2018). Higher-order sliding surface (Amini et al., 2017) and integral sliding surface (Integral SMC) (Norouzi et al., 2019c) were used to control nonlinear systems. SMC has been integrated with iterative learning based sliding surface to enhance SMC tracking performance of wire tension of an automatic motor winding machine control (Lu et al., 2018). An adaptive law was combined with ILC to design output reference tracking control for a class of nonlinear plants (Yan et al., 2018). Adaptive ILC was combined with non-singular fast terminal sliding mode, and second-order SMC was used to increase convergence speed. The experiment using a 6-DOF robotic manipulator results in increasing in convergence of controller by using second-order SMC and ILC combination (Wu et al., 2018).

In this research, PD-type Iterative Learning control (PD-ILC) combined with an Adaptive Sliding Mode Controller (ASMC) using a plug-in structure is used. Convergence and stability of the ILC controller are mathematically analyzed, and stability of SMC and ASMC are checked based on Lyapunov stability theory. Compared to a classic ILC controller, the proposed ASMC-PD-ILC controller improves the performance resulting in fast and accurate reference tracking control. The proposed controller is used to control a 2-DOF Quanser© QUBE^{TM} Servo 2 Rotary Pendulum.

2 System Model

Consider the Multi-Input-Multi-Output (MIMO) system dynamic model which has m inputs and p outputs as

$$\ddot{q} = f(q,\dot{q}) + g(q)\, u, \tag{1}$$

where q is the generalized coordinate vector, u is the input vector as

$$\begin{aligned} q &= [q_i]_{p\times 1} \quad i = 1,...,p \\ u &= [u_j]_{m\times 1} \quad j = 1,...,m. \end{aligned} \tag{2}$$

Now f and g are introduced as the uncertainty as

$$\begin{aligned} f &= [f_i]_{p\times 1} \quad i = 1,...,p \\ g &= [g_{ij}]_{p\times m} \quad i = 1,...,p,\ j = 1,...,m, \end{aligned} \tag{3}$$

where it is assumed that the minimum and maximum of f_i and g_{ij} are known and can be calculated as f_i^-, f_i^+, g_{ij}^-, and g_{ij}^+. The estimation of these functions and error of estimation are $\hat{f} = [\hat{f}_i]_{p\times 1}$, $\hat{g} = [\hat{g}_{ij}]_{p\times m}$, $\gamma = \gamma_{ij}$, $F = [F_i]_{p\times 1}$ and $G = [G_{ij}]_{p\times m}$ with the terms defined as

$$\begin{aligned} &\hat{f}_i = \frac{f_i^+ + f_i^-}{2},\ \ \hat{g}_{ij} = \sqrt{g_{ij}^+\, g_{ij}^-},\ \ \gamma_{ij} = \sqrt{\frac{g_{ij}^+}{g_{ij}^-}} \\ &F_i \geq |f_i^+ - \hat{f}_i| \ \ or \ \ F_i \geq |\hat{f}_i - f_i^-|. \end{aligned} \tag{4}$$

The system, linearized around a certain point, is defined in the state space form:

$$\dot{x}_{n\times 1} = A_{n\times n}x_{n\times 1} + B_{n\times m}u_{m\times 1}, \quad y_{p\times 1} = C_{p\times n}x_{n\times 1}, \tag{5}$$

where $x_{n\times 1}$, $y_{p\times 1}$, and $u_{m\times 1}$ are the model states, outputs, and inputs, respectively. The transfer function of system is calculated based on linearized system as

$$G_{sys}(s) = C[sI - A]^{-1}B, \tag{6}$$

where G_{sys} is the $p \times m$ transfer function matrix. For the remainder of the paper it is assumed the number of outputs equals the number of inputs ($p = m$).

3 Sliding Mode Control

For the system Eq. 1, the sliding surface is selected as

$$s = (\lambda + \frac{d}{dt})e = \lambda e + \dot{e}, \tag{7}$$

where λ is diagonal matrix including λ_{ii} ($i = 1,...,p$). The error vector of system is defined as

$$e = q - q_d \tag{8}$$

where $e = [e_i]_{p\times 1}$ and q_d is the desired reference input. The best control law for sliding mode controller is achieved by setting the time derivative of sliding surface equal to zero (Slotine et al., 1991). The time derivative of Eq. 7 is

$$\dot{s} = \lambda\dot{e} + \ddot{e} = 0, \tag{9}$$

and substituting Eq. 8 into Eq. 9 and solving results in:

$$\lambda\dot{q} - \lambda\dot{q}_d + \ddot{q} - \ddot{q}_d = 0, \tag{10}$$

where $\ddot{q}$ can be find by substituting $\hat{f}(q,\dot{q})$ and $\hat{g}(q)$ into Eq. 1 as (Slotine et al., 1991)

$$\ddot{q} = \hat{f}(q,\dot{q}) + \hat{g}(q)\, u_{eq}, \tag{11}$$

where u_{eq} is a control input which makes the derivative of sliding surface equal to zero. Substituting Eq. 11 into Eq. 10 results in

$$\lambda\dot{q} - \lambda\dot{q}_d + \hat{f}(q,\dot{q}) + \hat{g}(q)\, u_{eq} - \ddot{q}_d = 0. \tag{12}$$

Taking $u_{eq} = \hat{g}(q)^{-1}\hat{u}$ and solving Eq. 12 for $\hat{u}$ results in

$$\hat{u} = -\lambda\dot{q} + \lambda\dot{q}_d - \hat{f}(q,\dot{q}) + \ddot{q}_d. \tag{13}$$

The sliding condition is defined as

$$\frac{1}{2}\frac{d}{dt}s^T s \leq \eta||s||, \tag{14}$$

where η is a strictly positive diagonal matrix $\eta = [\eta_{ii}]_{p\times p}$ (Slotine et al., 1991). To satisfy the sliding condition, a switch term is added to u_{eq} as

$$u = u_{eq} - \hat{g}(q)^{-1}\, k\ sign(s), \tag{15}$$

where k is diagonal switching gain matrix. Now, $k\ sign(s)$ is defined as a diagonal matrix

$$k\ sign(s) = [k_{ii}]_{p\times p}\, [sign(s_i)]_{p\times 1}. \tag{16}$$

The sliding mode controller is obtained as

$$u_{SMC} = \hat{g}(q)^{-1}\Big(-\lambda\dot{e} - \hat{f}(q,\dot{q}) + \ddot{q}_d - k\ sign(s)\Big). \tag{17}$$

3.1 Adaptive Sliding Mode Control

An adaptive law can be added to update the switching gain based on the sliding surface (Norouzi et al., 2018) as

$$\dot{\hat{k}}_{ii}(t) = \beta_{ii}\ |s_i(t)|,\ \ \hat{k}_{ii}(t|_{t=0}) = 0, \tag{18}$$

where in the matrix format it can be defined as

$$\dot{\hat{k}}(t) = \beta\ |s(t)|,\ \ \hat{k}(t|_{t=0}) = 0, \tag{19}$$

where β is the diagonal matrix of elements β_{ii}. So, the adaptive sliding mode controller is calculated as

$$u_{ASMC} = \hat{g}(q)^{-1}\Big(-\lambda\dot{e} - \hat{f}(q,\dot{q}) + \ddot{q}_d - \hat{k}\ \beta\ sign(s)\Big), \tag{20}$$

where now $\hat{k}$ is a function of time.

4 PD-type Iterative Learning Control (PD-ILC)

Iterative Learning Control is often defined as

$$u_{j+1}(t) = Q(u_j(t)) + L(e_j(t)), \tag{21}$$

where L is a learning filter, Q is a Q-Filter (Control input filter), and j is cycle index. Both Q and L are matrices with dimension of $p \times p$. If the learning filter has only constant values on the main diagonal elements of matrix, then a the P-type controller is generated. Taking Q to be a identity matrix results in (Ahn et al., 2007)

$$u_{j+1}(t) = u_j(t) + Le_j(t), \tag{22}$$

where the current cycle control input is function of the previous cycle's error and control input. By modifyng the matrix L a PD-type ILC controller is obtained as

$$u_{j+1}(t) = u_j(t) + Pe_j(t) + D\dot{e}_j(t), \tag{23}$$

where P and D is the proportional and derivative learning gain, respectively (Ahn et al., 2007).

5 Hybrid Plug-in PD-type ILC with ASMC- ASMC-PD-ILc

The Plug-in ILC with parallel structure is (Lei et al., 2015)

$$u_j(t) = u_{ASMC,j}(t) + u_{PD-ILC,j}(t), \tag{24}$$

where $u_{ASMC,j}(t)$ is the ASMC controller, $u_{PD-ILC,j}(t)$ is the PD-type ILC, $u_j(t)$ is the combined control signal of the system, and j is iteration cycle. The proposed hybrid controller block diagram is shown schematically in Fig. 1. Substituting Eq. 23 and 20 into Eq. 24 the hybrid control law is calculated as

$$\begin{aligned} u_j = \hat{g}^{-1}(q_j)\Big(&-\lambda\dot{e}_j - \hat{f}(q_j,\dot{q}_j) + \ddot{q}_d - \hat{k}\ \beta\ sign(s_j)\Big) \\ &+ u_{j-1} + Pe_{j-1} + D\dot{e}_{j-1}. \end{aligned} \tag{25}$$

To avoid chattering, a saturation function with constant boundary layer is used instead of the $[sign(s_i)]_{p\times 1}$ function as

$$sat(\frac{s_i}{\phi}) = \begin{cases} 1 & \frac{s_i}{\phi} > 1 \\ \frac{s_i}{\phi} & -1 < \frac{s_i}{\phi} < 1 \\ -1 & \frac{s_i}{\phi} < -1 \end{cases} \quad i = 1,...,n \tag{26}$$

6 Stability Analysis

6.1 Stability Analysis of ILC controller

The term $Q - G_{sys}L$ is used as the stability criteria to analysis the stability of an ILC controller for a linear system. So, for ILC asymptotic stability, a necessary but not sufficient conditions for this case is defined as

$$||Q - G_{sys}L||_\infty < 1, \tag{27}$$

or $\bar{\sigma}(Q - G_{sys}L) < 1$ where L is a diagonal matrix and G_{sys} is a symmetric matrix, and $\bar{\sigma}$ is a maximum singular value (Owens, 2015). Monotonic convergence occurs when $\bar{\sigma}(M) < 1$ where $M = [Q - G_{sys}(s)L]$ in $e_{j+1} = Me_j$. Using the same concept for convergence and stability analysis of P-type ILC, the stability and convergence criteria for PD-type ILC can be calculated as

$$\begin{aligned} e_{j+1} &= q_d - y_{j+1} = r - G_{sys}u_{j+1} \\ &= q_d - G_{sys}Qu_j - G_{sys}Pe_j - sG_{sys}De_j. \end{aligned} \tag{28}$$

So, by assuming that the Q-filter equals to identity matrix, M is calculated as

$$e_{j+1}(s) = [I - G_{sys}(s)(P + sD)]e_j(s). \tag{29}$$

Thus, for the PD-type controller stability and convergence conditions are

$$\bar{\sigma}(I - G_{sys}(s)(P + sD)) < 1. \tag{30}$$

The second norm of error can be calculated as

$$||e_{q(j)}||_2 = \sqrt{e^*_{q(j)}e_{q(j)}}, \tag{31}$$

where j is the repetitive cycle number and e_q is the tracking error vector of q in Eq. 8.

6.2 Adaptive Sliding Mode control

To establish the sliding condition (Eq. 14), the range of k is found to be

$$k \geq \gamma\,(F + \eta) + (\gamma - I)\,|\hat{u}|, \tag{32}$$

where this equation is obtained based on Lyapunov stability theorem (Slotine et al., 1991) for SMC. For the stability analysis of ASMC a candidate Lyapunov function is defined as

$$V(t) = \frac{1}{2}s^T s + \frac{\hat{g}^{-1}g}{2}\tilde{k}^T\tilde{k}, \tag{33}$$

where $\tilde{k}$ is defined as

$$\tilde{k} = \hat{k} - k. \tag{34}$$

Taking the time derivative of candidate Lyapunov function (Eq. 33) and substituting the system dynamic model (Eq. 1) and ASMC control law (Eq. 20) results in

$$\begin{aligned} \dot{V}(t) &= s\dot{s} + \hat{g}^{-1}g\tilde{k}\dot{\tilde{k}} \\ &= s(\ddot{q} - \ddot{q}_d + \lambda\dot{e}) + \hat{g}^{-1}g(\hat{k} - k)\beta|s| \\ &= s(f + gu - \ddot{q}_d + \lambda\dot{e}) + \hat{g}^{-1}g(\hat{k} - k)\beta|s| \\ &= s(f + g\hat{g}^{-1}\big(-\lambda\dot{e} - \hat{f} + \ddot{q}_d - \hat{k}\,\beta\,sign(s)\big) \\ &\quad - \ddot{q}_d + \lambda\dot{e}) + \hat{g}^{-1}g(\hat{k} - k)\beta|s| \\ &= s(f - \hat{f} + \hat{f} + g\hat{g}^{-1}\big(-\lambda\dot{e} - \hat{f} + \ddot{q}_d - \hat{k}\,\beta\,sign(s)\big) \\ &\quad - \ddot{q}_d + +\lambda\dot{e}) + \hat{g}^{-1}g(\hat{k} - k)\beta|s| \\ &= s\big((f - \hat{f}) + (g\hat{g}^{-1} - 1)(-\hat{f} + \ddot{q}_d - +\lambda\dot{e}) \\ &\quad - g\hat{g}^{-1}\hat{k}sign(s)\big) + g\hat{g}^{-1}(\hat{k} - k)\beta|s|. \end{aligned}$$

simplifying using the triangle inequality and using Eq. 4, results in

$$\dot{V}(t) \leq |s||F| + |s||g\hat{g}^{-1} - 1||\hat{u}| - g\hat{g}^{-1}k\beta|s|. \tag{35}$$

Based on Eq. 4, $|1 - g\hat{g}^{-1}| \leq |1 - \gamma^{-1}|$ and $-g\hat{g}^{-1} \leq -\gamma^{-1}$ are obtained. Then, substituting these into the Eq. 35 results in

$$\dot{V}(t) \leq |s||F| + |s||1 - \gamma^{-1}||\hat{u}| - \gamma^{-1}k\beta|s|. \tag{36}$$

Finally, substituting Eq. 32 into Eq. 36, results in

$$\begin{aligned} \dot{V}(t) &\leq |s||F| + |s||1 - \gamma^{-1}||\hat{u}| \\ &\quad - \gamma^{-1}(\gamma\,(F + \eta) + (\gamma - I)\,|\hat{u}|)\beta|s| \\ &\leq \big((I - \beta)(F + |I - \gamma^{-1}||\hat{u}|)|s|\big) - \eta\beta|s|. \end{aligned} \tag{37}$$

So, if $\beta_i \geq 1$ the time derivative of Lyapunov function would be $\dot{V}(t) \leq 0$. So, the system is stable based on Lyapunov stability theory, if and only if $\beta_i \geq 1$ for all i.

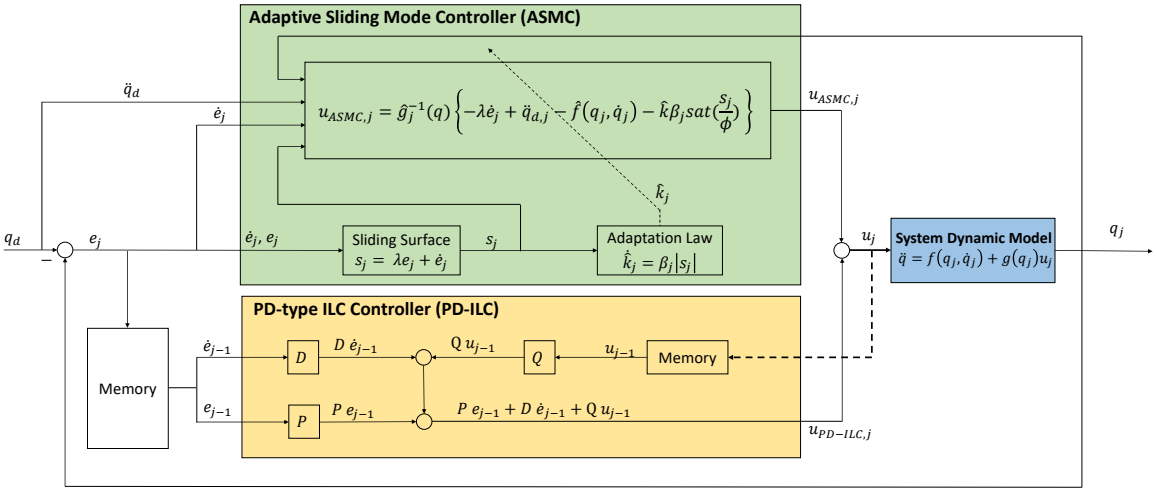

Fig. 1. Hybrid Adaptive Sliding Mode Control with PD-type Iterative Learning Control (ASMC-PD-ILC)

7 Experiment Results and Discussion

To experimentally test the proposed controller, the Quanser© QUBE^{TM} Servo 2 rotary pendulum is used. A schematic of system is shown in Fig. 2. Using the Euler-Lagrange method, the dynamic model of system is obtained as (Apkarian et al., 2016)

$$\begin{bmatrix} M_{11} & M_{12} \\ M_{21} & M_{22} \end{bmatrix} \begin{bmatrix} \ddot{\theta} \\ \ddot{\alpha} \end{bmatrix} + \begin{bmatrix} C_1 \\ C_2 \end{bmatrix} = \begin{bmatrix} T_1 \\ T_2 \end{bmatrix}, \tag{38}$$

where

$$M_{11} = m_p L_r^2 + \frac{1}{4} m_p L_p^2 - \frac{1}{4} m_p L_p^2 \cos(\alpha)^2 + J_r$$

$$M_{12} = \frac{1}{2} m_p L_p L_r \cos(\alpha),\ M_{21} = \frac{1}{2} m_p L_p L_r \cos(\alpha)$$

$$M_{22} = J_p + \frac{1}{4} m_p L_p^2,\ C_1 = \left(\frac{1}{2} m_p L_p^2 \sin(\alpha)\cos(\alpha)\right)\dot{\theta}\dot{\alpha} + \left(\frac{1}{2} m_p L_p L_r \sin(\alpha)\right)\dot{\alpha}^2 + \frac{k_m^2 \dot{\theta}}{R_m} + D_r$$

$$C_2 = -\frac{1}{4} m_p L_p \cos(\alpha)\sin(\alpha)\dot{\theta}^2 + \frac{1}{2} m_p L_p g \sin(\alpha) + D_p \dot{\alpha}.$$

The right hand of Eq. 38 is the input torque to the first and second link defined as $[B_1 \ \ B_2]^T V_m$ where $B_1 = K_m/R/m$ and $B_2 = 0$. The DC motor voltage (V_m) is control input (actuator dynamic is included) and rotary link angle (θ) and pendulum angle (α) are system outputs. The experimental setup using QUBE rotary Pendulum is shown in Fig. 3. Based on Eq. 38, the standard for of dynamic equation of motion (Eq. 1) as achieved where $f(q,\dot{q})$, $g(q)$, q, and u are defined as

$$q = [\theta\ \alpha]^T,\ u = V_m,$$
$$f(q,\dot{q}) = -[M]^{-1}C,\ g(q) = [M]^{-1}B.$$

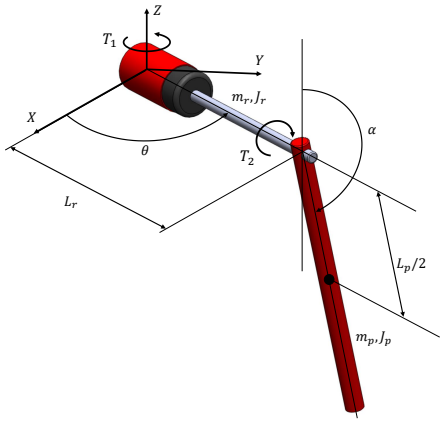

Fig. 2. kinematic diagram of the QUBE rotary pendulum

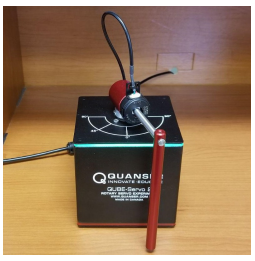

Fig. 3. Experiment setup of QUBE rotary pendulum

Fig. 4 shows the experimental results of SMC and ASMC controllers. In all experimental results a back and forth reference desired input is used as rotary desired angle (θ) and 180° reference desired input for pendulum angle (α). Reference tracking results of SMC versus ASMC show the adaptation law in the SMC controller results in more accurate reference tracking in Fig. 4. Adding an adaptive law decreases second norm of error for one single cycle from 18.74 for SMC to 12.43 for ASMC. The more accurate tracking of rotary angle (θ) using ASMC, the more oscillatory the pendulum angle (α). The experimental result of PD-ILC controller for repetitive reference of rotary angle (α) are shown in Fig. 5. In this test, a square Wave with amplitude of 20 degree and frequency of 0.0625 Hz is used as reference input and each period of this square wave is taken as a cycle for PD-ILC controller. As illustrated, after a 31 cycles, the controller can achieve acceptable tracking of desired reference. This is quantified by the second norm of error of each cycle versus number of iteration ($||e_\theta||_2$ versus j plot in Fig. 5) where shows ILC monotonic convergence. The experimental results of reference tracking using Hybrid ASMC-PD-ILC controller are shown in Fig. 6 . The reference input is the same as Fig. 5. For this case, the combined controller converges faster than pure ILC controller and second norm of the error decreases from 23.67 to 9.69.

As shown in Figs. 4-6, the damping between the joint of rotatory arm and pendulum is very low. Hence, by increasing the tracking accuracy and response time of the θ , the oscillation on the α increases. This is a trade-off between tracking the desired value of the θ and stabilizing the pendulum ($\theta = 180°$). Based on Fig. 6, from cycle 1 to 7, oscillation is increased as the response time, and the accuracy of θ tracking is increased. For the last four cycles, both oscillation, and θ tracking stays unchanged. This can be analyzed based on the second norm of error ($||e_\theta||$), as shown in Fig. 6. At convergence of the learning control, the performance remains unchanged as the reference is repeated with the same amplitude and frequencies. The same conclusion can be made for pure ILC controller as shown in Fig. 5.

To compare performance of different controller, the second norm of tracking error of last cycle is compared in Table 1. Also, the last cycle of system response for four kinds of controllers are shown in Fig. 7.

Table 1. Performance comparison of controllers

Controller type	$\|\|e_\theta\|\|_2$	Accuracy wrt SMC	Accuracy wrt ILC
SMC	18.74	-	-32.9%
ASMC	12.43	+33.7%	+1.1%
ILC	12.57	+32.9	-
ILC with ASMC	9.68	+48.3%	+23%

Based on Table 1, it can be concluded that the proposed combined controller has faster convergence and more accurate reference tracking than PD-type ILC controllers. The proposed controller converges in 11 cycles while for pure ILC the convergence occurs in 31 cycles (64.5% faster). The combined controller is also an improvement on just the ASMC. The combination of ASMC-PD-ILC produces the best results when compared to the individual controllers.

8 Conclusion

A PD-type Iterative Learning Controller is combined with Adaptive Sliding Mode Controller and the stability and convergence of the proposed controller are analyzed. Then, a 2-DOF QUBE rotary pendulum is used to test the designed controllers

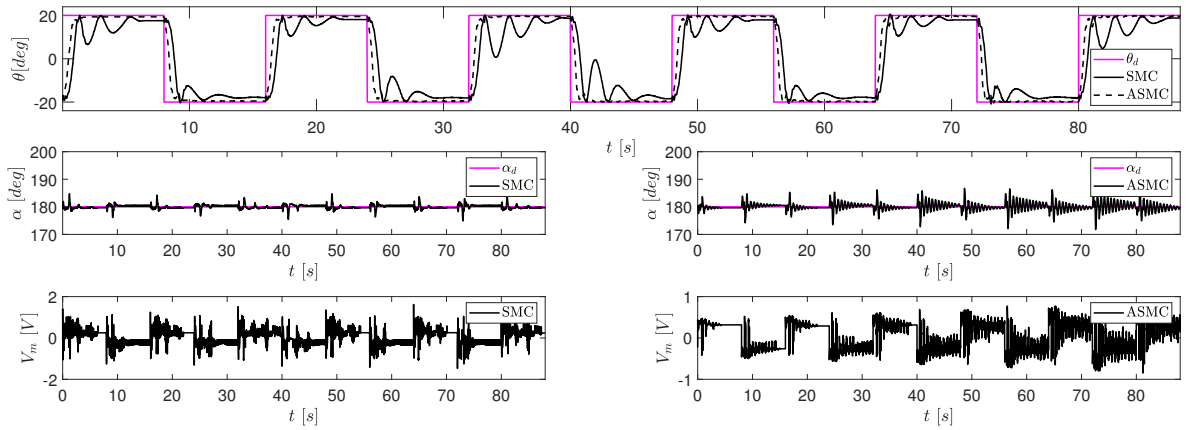

Fig. 4. Experimental results: reference tracking of QUBE rotary angle (θ) and stabilizing pendulum angle (α) using Sliding Mode Controller (SMC) versus Adaptive Sliding Mode Controller (ASMC)

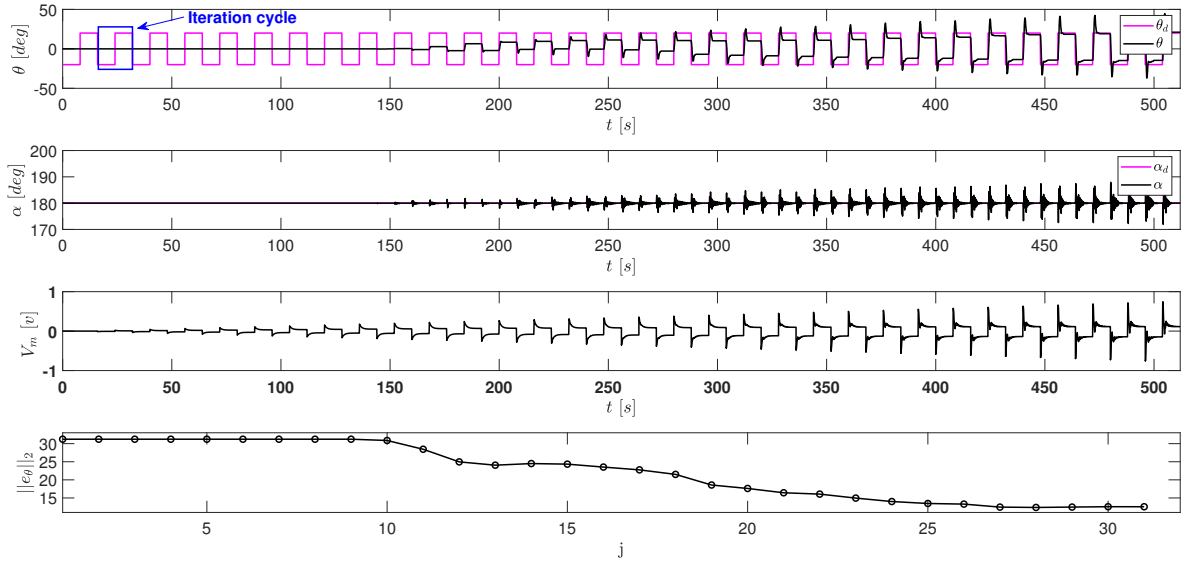

Fig. 5. Experimental results: reference tracking of QUBE rotary angle (θ) and stabilizing pendulum angle (α) using PD-type Iterative Learning Control (PD-ILC)

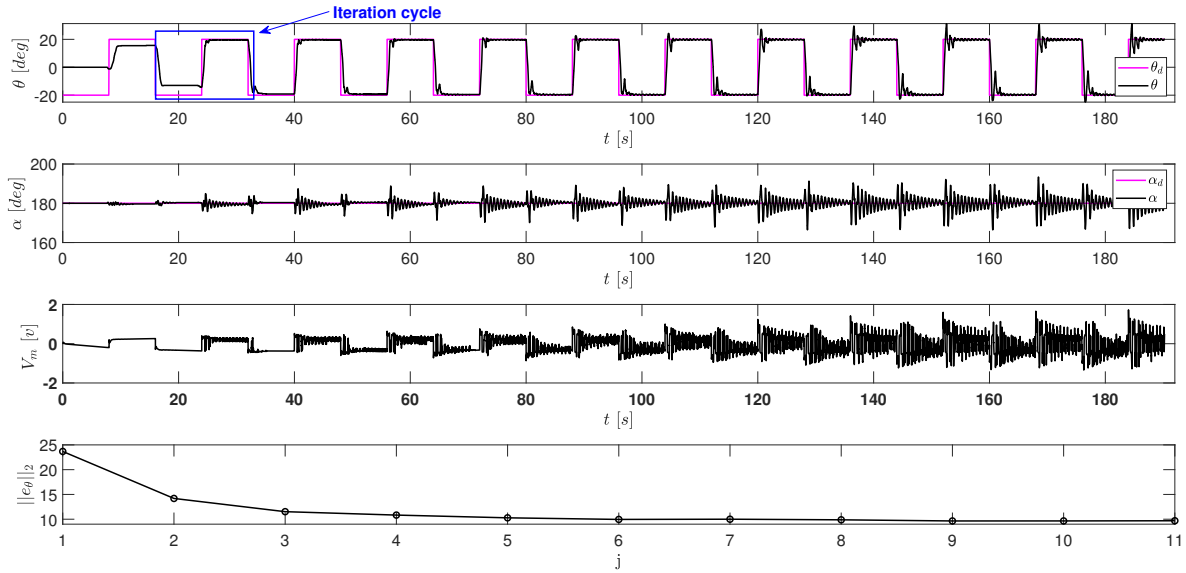

Fig. 6. Experimental results: reference tracking of QUBE rotary angle (θ) and stabilizing pendulum angle (α) using Hybrid Adaptive Sliding Mode Controller and PD-type Iterative Learning Control (ASMC-PD-ILC)

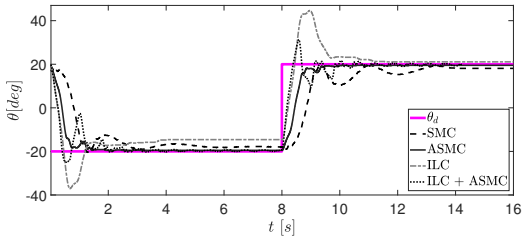

Fig. 7. Performance comparison of controllers - the last cycle of learning-based controller are considered for comparison

by comparing experimental results of SMC and ASMC, PD-ILC, and ASMC-PD-ILC. For this system several observation can be made. One, adding the adaptation law helps the hybrid controller to achieve more accurate tracking performance. Two, adding ASMC to PD-ILC improves system convergence speed and tracking performance. Three, as the ASMC controller is designed based on the model, it depends on the accuracy of the model; however, the proposed controller is able to compensate model mismatch of plant system model to improve tracking accuracy of the controller. This is clear by using adaptation and learning together. Understanding how the additional methods such as Backstepping Control, Model Predictive Control, and Optimal Control could be added to further improve the control performance is future research.

References

Ahn, H.S., Chen, Y., and Moore, K.L. (2007). Iterative learning control: Brief survey and categorization. *IEEE Transactions on Systems, Man, and Cybernetics, Part C (Applications and Reviews)*, 37(6), 1099–1121.

Amini, M.R., Shahbakhti, M., Pan, S., and Hedrick, J.K. (2017). Discrete adaptive second order sliding mode controller design with application to automotive control systems with model uncertainties. In *2017 American Control Conference (ACC)*, 4766–4771. IEEE.

Apkarian, J., Levis, M., and Martin, P. (2016). *QUBE-Servo 2 Workbook (Student): Experiment for MATLAB/Simulink Users*. Quanser Inc.

Dong, J., He, B., Ming, M., Zhang, C., and Li, G. (2019). Design of open-closed-loop iterative learning control with variable stiffness for multiple flexible manipulator robot systems. *IEEE Access*, 7, 23163–23168.

He, W., Meng, T., He, X., and Sun, C. (2018). Iterative learning control for a flapping wing micro aerial vehicle under distributed disturbances. *IEEE transactions on cybernetics*, 49(4), 1524–1535.

Hofer, M., Spannagl, L., and D'Andrea, R. (2019). Iterative learning control for fast and accurate position tracking with a soft robotic arm. *arXiv preprint arXiv:1901.10187*.

Jiang, B., Karimi, H.R., Kao, Y., and Gao, C. (2018). A novel robust fuzzy integral sliding mode control for nonlinear semi-markovian jump t–s fuzzy systems. *IEEE Transactions on Fuzzy Systems*, 26(6), 3594–3604.

Khalil, H.K. (2002). Nonlinear systems. *Upper Saddle River*.

Kim, D.I. and Kim, S. (1996). An iterative learning control method with application for CNG machine tools. *IEEE Transactions on Industry Applications*, 32(1), 66–72.

Lei, Z., Baichen, Z., Dengyun, W., and Ming, L. (2015). A low speed servo system of CMG gimbal based on adaptive sliding mode control and iterative learning compensation. In *2015 IEEE International Conference on Mechatronics and Automation (ICMA)*, 2249–2254. IEEE.

Liu, Y. and Ruan, X. (2018). Spatial iterative learning control for pitch of wind turbine. In *2018 IEEE 7th Data Driven Control and Learning Systems Conference (DDCLS)*, 841–846. IEEE.

Lu, J.S., Cheng, M.Y., Su, K.H., and Tsai, M.C. (2018). Wire tension control of an automatic motor winding machinean iterative learning sliding mode control approach. *Robotics and Computer-Integrated Manufacturing*, 50, 50–62.

Norouzi, A., Aliramezani, M., and Koch, C.R. (2019a). Diesel engine NOx reduction using a PD-type fuzzy iterative learning control with a fast response NOx sensor. *Proceedings of Combustion Institute-Canadian Section*.

Norouzi, A., Barari, A., and Adibi-Asl, H. (2019b). Stability control of an autonomous vehicle in overtaking manoeuvre using wheel slip control. *International Journal of Intelligent Transportation Systems Research*.

Norouzi, A., Ebrahimi, K., and Koch, C.R. (2019c). Integral discrete-time sliding mode control of homogeneous charge compression ignition (HCCI) engine load and combustion timing. In *9th Symposium on Advances in Automotive Control (AAC 2019)*. IFAC.

Norouzi, A., Kazemi, R., and Azadi, S. (2018). Vehicle lateral control in the presence of uncertainty for lane change maneuver using adaptive sliding mode control with fuzzy boundary layer. *Proceedings of the Institution of Mechanical Engineers, Part I: Journal of Systems and Control Engineering*, 232(1), 12–28.

Norouzi, A. and Koch, C.R. (2019). Robotic manipulator control using PD-type fuzzy iterative learning control. In *2019 IEEE Canadian Conference on Electrical & Computer Engineering (CCECE)*. IEEE.

Norouzi, A., Masoumi, M., Barari, A., and Farrokhpour Sani, S. (2019d). Lateral control of an autonomous vehicle using integrated backstepping and sliding mode controller. *Proceedings of the Institution of Mechanical Engineers, Part K: Journal of Multi-body Dynamics*, 233(1), 141–151.

Owens, D.H. (2015). *Iterative learning control: an optimization paradigm*. Springer.

Slepicka, C. and Koch, C.R. (2016). Iterative learning on dual-fuel control of homogeneous charge compression ignition. *IFAC-PapersOnLine*, 49(11), 347–352.

Slotine, J.J.E., Li, W., et al. (1991). *Applied nonlinear control*, volume 199. Prentice hall Englewood Cliffs, NJ.

Wu, S., Wu, A., Dong, N., and Dong, Q. (2018). Adaptive iterative learning control of robotic manipulator with second-order terminal sliding mode method. In *2018 13th World Congress on Intelligent Control and Automation (WCICA)*, 1488–1493. IEEE.

Xu, J.X., Panda, S.K., and Lee, T.H. (2008). *Real-time iterative learning control: design and applications*. Springer Science & Business Media.

Xu, J.X., Tan, Y., and Lee, T.H. (2004). Iterative learning control design based on composite energy function with input saturation. *Automatica*, 40(8), 1371–1377.

Yan, Q., Cai, J., Ma, Y., and Yu, Y. (2019). Robust learning control for robot manipulators with random initial errors and iteration-varying reference trajectories. *IEEE Access*, 7, 32628–32643.

Yan, Q., Cai, J., Yu, Y., and Ma, Y. (2018). Recursive sliding mode based iterative learning control. In *2018 5th International Conference on Information, Cybernetics, and Computational Social Systems (ICCSS)*, 343–347. IEEE.